



A Journal of the Gesellschaft Deutscher Chemiker

Angewandte Chemie

GDCh

International Edition

www.angewandte.org

Accepted Article

Title: Solvent adaptive dynamic metal-organic soft hybrid for imaging and biological delivery

Authors: Debabrata Samanta, Syamantak Roy, Ranjan Sasmal, Nilanjana Das Saha, Pradeep K R, Ranjani Viswanatha, Sarit S. Agasti, and Tapas Kumar Maji

This manuscript has been accepted after peer review and appears as an Accepted Article online prior to editing, proofing, and formal publication of the final Version of Record (VoR). This work is currently citable by using the Digital Object Identifier (DOI) given below. The VoR will be published online in Early View as soon as possible and may be different to this Accepted Article as a result of editing. Readers should obtain the VoR from the journal website shown below when it is published to ensure accuracy of information. The authors are responsible for the content of this Accepted Article.

To be cited as: *Angew. Chem. Int. Ed.* 10.1002/anie.201900692
Angew. Chem. 10.1002/ange.201900692

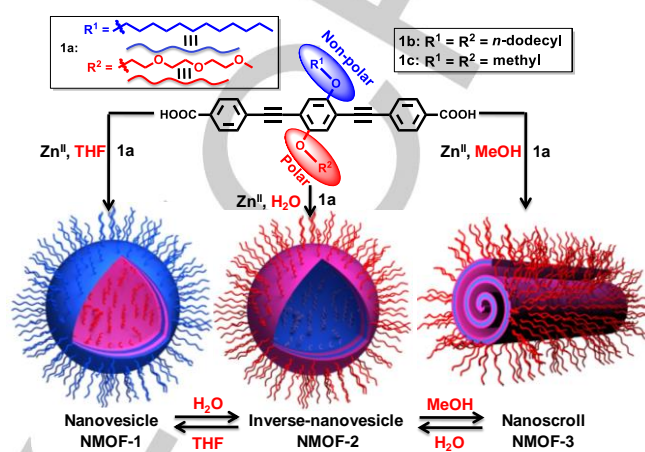
Link to VoR: <http://dx.doi.org/10.1002/anie.201900692>
<http://dx.doi.org/10.1002/ange.201900692>

COMMUNICATION

Solvent adaptive dynamic metal-organic soft hybrid for imaging and biological delivery

Debabrata Samanta,^a Syamantak Roy,^a Ranjan Sasmal,^b Nilanjana Das Saha,^b Pradeep K R,^b Ranjani Viswanatha,^{bc} Sarit S. Agasti,^{ab} Tapas Kumar Maji^{*abc}

Abstract: A solvent responsive dynamic nanoscale metal-organic framework (NMOF) $[Zn(1a)(H_2O)_2]$ has been devised based on the self-assembly of Zn^{II} and asymmetric bola-amphiphilic *oligo*-(*p*-phenyleneethynylene) (OPE) dicarboxylate linker **1a** having dodecyl and triethyleneglycolmonomethylether (TEG, polar) side chains. In THF solvent, NMOF showed nanovesicular morphology (**NMOF-1**) with surface decorated dodecyl chains. In water and methanol, NMOF exhibited inverse-nanovesicle (**NMOF-2**) and nanoscroll (**NMOF-3**) morphology, respectively, with surface projected TEG chains. The pre-formed NMOFs also unveiled reversible solvent responsive transformation of different morphologies. The flexible NMOF showed cyan emission and no cytotoxicity, allowing live cell imaging. Cisplatin (14.4 wt%) and doxorubicin (4.1 wt%) were encapsulated in **NMOF-1** by non-covalent interactions and, in-vitro and in-vivo drug release was studied. The drug loaded NMOFs exhibited micromolar cytotoxicity.



Scheme 1. Schematic representation of synthesis and morphology transformation of NMOFs.

The recent upsurge in design and synthesis of meso/nanoscale metal-organic frameworks (MOFs) stems from their solution processability.^[1] This has magnified the landscape of application of MOFs in several interdisciplinary areas, particularly in biology^[2] and device fabrication.^[3] Several synthetic methodologies and approaches have been adopted to fabricate nanoscale MOFs (NMOFs) with varied shape, size and morphologies.^[4] However, fabrication of solvent responsive chromophoric NMOFs with flexible and dynamic morphologies, based on a suitable linker, is yet to be explored. Such tailoring of MOF nanostructure will find potential applications in drug delivery,^[5] molecular recognition and sensing^[6] or separation of specific molecules.^[7] So far, Fe, Zr, and Zn MOFs have been found to be bio-compatible and frequently utilized as nanocarriers for drug delivery.^[8] Recently, our group has adopted a strategy towards the synthesis of nano/mesoscale MOFs with varied morphologies by self-assembly of bola-amphiphilic *oligo-p*-phenyleneethynylene carboxylate (OPE) based chromophoric linker with different metal ions.^[9] The dynamic nanostructures obtained by tuning the length of alkyl chains in OPE linkers showed applications in light harvesting,

bimodal imaging, sensing, photocatalysis and also as a superhydrophobic self-cleaning material.^[9] The introduction of different polarity like glycol and alkyl chain on the OPE backbone, will result in asymmetric bola-amphiphilicity and we envisioned that self-assembly of such linker with specific metal ions will result in NMOFs with omniphilic pore surfaces. Such modulation of the polarity of pore surfaces is of paramount importance for encapsulation of suitable molecular species or drug molecules.^[10] Furthermore, polarity and philicity of the outer surface of the preformed NMOFs can also be tuned based on the polarity of the solvent media. Fabrication of such luminescent, reversible shape shifting dynamic NMOFs are yet to be documented and can be applied in bioimaging and drug delivery.

In this communication, we report the self-assembly of bola-amphiphilic asymmetric organic linker (OPE, **1a**) with Zn^{II} to form three reversibly shape shifting and non-toxic NMOFs with nanovesicle (**NMOF-1**), inverse nanovesicle (**NMOF-2**) and nanoscroll (**NMOF-3**) morphologies. The emissive nature of the NMOFs allowed for bio-imaging applications. Furthermore, the omniphilicity of the pores of **NMOF-1** was utilized for cisplatin and doxorubicin drug loading and their subsequent in vitro and in vivo release study.

The nanoscale metal-organic framework, **NMOF-1** was prepared by mixing Zn^{II} and the linker **1a** (1:1) in THF under basic condition. Inductively coupled plasma atomic emission spectroscopy (ICP-AES) and energy-dispersive X-ray spectroscopy (EDAX) showed the presence of 8.12 wt% and 7.91 wt% of Zn, respectively (Figure S1). Fourier transform IR spectroscopy (FT-IR) showed the signature of Zn^{II} coordinated water molecules at 3400 cm^{-1} (Figure S2). The symmetric and asymmetric stretching frequencies of carboxylate were found at 1592 and 1399 cm^{-1} , respectively, indicating coordination of carboxylate with Zn^{II} . Thermogravimetric analysis (TGA) revealed an initial weight loss of 4.5 wt% which continued upto $210\text{ }^{\circ}\text{C}$

- [a] Dr. D. Samanta, Dr. S. Roy, Prof. Dr. S. S. Agasti, Prof. Dr. T. K. Maji, Chemistry and Physics of Materials Unit, School of Advanced Materials (SAMat), Jawaharlal Nehru Centre for Advanced Scientific Research (JNCASR), Jakkur, Bangalore-560064, India. E-mail: tmaji@jncasr.ac.in
- [b] R. Sasmal, Pradeep K. R., Dr. N. D. Saha, Prof. Dr. S. S. Agasti, Prof. Dr. R. Viswanatha, Prof. Dr. T. K. Maji, New Chemistry Unit and School of Advanced Materials (SAMat), Jawaharlal Nehru Centre for Advanced Scientific Research (JNCASR), Jakkur, Bangalore-560064, India
- [c] Prof. Dr. T. K. Maji, Prof. Dr. R. Viswanatha, International Centre for Materials Science, School of Advanced Materials (SAMat) Jawaharlal Nehru Centre for Advanced Scientific Research, Jakkur, Bangalore - 560064, India

Supporting information for this article is given via a link at the end of the document. ((Please delete this text if not appropriate))

COMMUNICATION

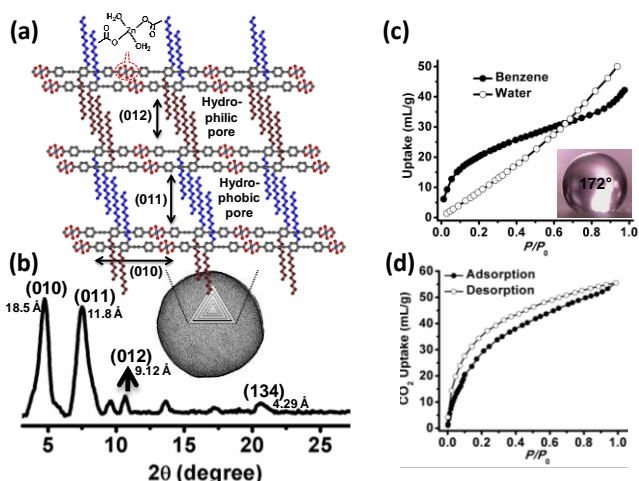


Figure 1. a) Possible packing and b) PXRD pattern of the **NMOF-1**. c) Benzene and water vapour adsorption isotherms of **NMOF-1** (295 K) (inset: water contact angle), and d) CO_2 adsorption profile of **NMOF-1** at 195 K.

possibly due to removal of Zn(II) -coordinated two water molecules (Figure S3). In combination with elemental analysis, EDAX, ICP and TGA, the molecular formula of the MOF was determined to be $\text{Zn}(\mathbf{1a}) \cdot 2\text{H}_2\text{O}$ i.e. linker **1a** and Zn^{II} are complexed in 1:1 ratio and two water molecules are seemingly coordinated to each Zn^{II} . To understand the coordination environment of **NMOF-1**, Zn K-edge EXAFS study was performed and quick shell fitting showed that the coordination number of Zn^{II} is ~ 4 (Figure S4, Table S1). This suggests Zn^{II} is in a tetrahedral geometry with two water and two carboxylate oxygen atoms in **NMOF-1**. Powder X-ray diffraction (PXRD) measurement of **NMOF-1** showed high degree of crystallinity with several intense peaks corresponding to the d -spacing of 18.5 Å, 11.8 Å, 9.12 Å and 4.29 Å (Figure 1b). For instance, the most intense peak with a d -spacing at 18.5 Å indicates the repeating OPE-backbone that complexed with Zn^{II} forming a linear polymer (Figure 1a and Scheme S4). The broad pattern at 4.29 Å, represents that the linear 1D chains are extended in two-dimension via weak π -stacking. Another two peaks at 11.8 Å and 9.12 Å, can be understood as repeating units formed alternatively by dispersive interaction between dodecyl chains and hydrogen bonding between TEG chains, respectively (Figure 1a). The interdigitation between 2D layers resulted in a 3D supramolecular framework of **NMOF-1**. Indexing of the PXRD patterns showed an orthorhombic crystal system with cell parameters of $a = 9.67(2)$ Å, $b = 18.26(4)$ Å, $c = 31.38(7)$ Å and cell volume of 5544 Å³ (Table S2). The permanent porosity of **NMOF-1** was identified by the adsorption isotherms of N_2 (at 77 K) and CO_2 (at 195 K) with a final uptake of 26 cc/g and 55 cc/g, respectively, at $p = 1$ (Figure 1d/S5). N_2 adsorption showed type-II profile whereas CO_2 adsorption exhibited typical type-I profile which suggested microporosity in **NMOF-1**. Thus CO_2 adsorption occurred in the pore channel but N_2 adsorption took place in the inter-particle void space. The CO_2 adsorption profile validated 3D supramolecular arrangement of **NMOF-1**.

Morphology of **NMOF-1** was investigated by field emission scanning electron microscopy (FESEM) and transmission electron microscopy (TEM). All the microscopic analyses support nanovesicular morphology of **NMOF-1** with

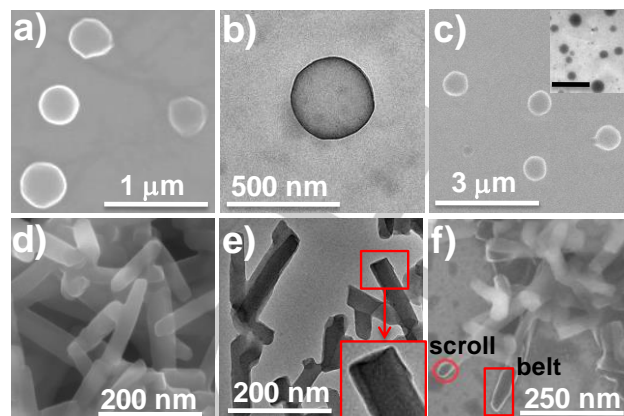


Figure 2. a) FESEM and b) TEM images of **NMOF-1**. c) FESEM and TEM (inset, scale bar: 2 μm) images of **NMOF-2**. d) FESEM and e) TEM images of **NMOF-3**. f) FESEM images of **NMOF-3** (1h).

diameter range of 100 – 400 nm (Figure 2a,b,S7,S8). An approximate wall thickness of the nanovesicles was found to be 5.7 ± 0.6 nm from the peripheral dark regions of TEM images (Figure S8), suggesting that the walls of the nanovesicles consist of 5 - 6 interdigitated layers (Figure 1a). As the NMOF is assembled by weak supramolecular interactions like π -stacking, H-bonding and van der Waals interactions, the morphology varied greatly on the polarity of solvent used for synthesis. For example, in polar water and moderately polar methanol medium, the formed NMOFs, namely **NMOF-2** and **NMOF-3**, showed inverse-nanovesicular and nanoscroll morphology, respectively, as observed in FESEM and TEM study (Figure 2, S9-S12). **NMOF-2** has diameter upto 700 nm and **NMOF-3** has wide distribution of length starting from 100 nm to 500 nm and diameter 50-60 nm. Sharp contrast for the openings of the nanoscroll was also observed (Figure 2f/S12). FT-IR spectroscopy, TGA, EDAX, ICP and elemental analysis concluded the molecular formula of **NMOF-2** and **NMOF-3** to be $\text{Zn}(\mathbf{1a})(\text{H}_2\text{O})_2$ which is the same as **NMOF-1** (Figure S2,S3,S13,S14). Notably, PXRD of **NMOF-2&3** are similar to that of **NMOF-1**, suggesting that the repeating OPE backbone and interdigitation are similar in all cases (Figure S15). The CO_2 uptake (195 K, $p = 1$) of **NMOF-2** and **NMOF-3** was found to be 44.6 cc/g and 46.4 cc/g, respectively, indicating their similarity in packing and pore structure (Figure S16).

As the linker **1a** contains mixed polar side chains, either dodecyl chains or TEG chains can be present on the outer surface of vesicles, depending on polarity of the solvent used for NMOF synthesis, and this arrangement was corroborated by comparing nonpolar and polar solvent vapor adsorption isotherms as well as water contact angle measurement. Benzene and water vapor adsorptions (at 295 K) were measured with activated samples of all three NMOFs. **NMOF-1-3** showed gradual uptake of both the solvents, indicating the presence of omniphilic pore surface (Figure 1c, S17/18). Strikingly, in the case of **NMOF-1**, benzene uptake is higher than water in the low pressure region $p = 0 - 0.63$, this may be due to hydrophobic nature of the exterior surface. The **NMOF-1** coated glass surface also showed superhydrophobic water contact angle of 172° whereas hexane droplet was found to be immediately spreading over the surface. As the synthesis of **NMOF-1** was performed in THF, the dodecyl chains got exposed on the outer surface of the nanovesicles, resulting in the

COMMUNICATION

superhydrophobic surface. The measured water contact angle on **NMOF-2** and **NMOF-3** coated glass surfaces are 55 and 74°, respectively, representing hydrophilic exterior surface due the projection of TEG chains in both the NMOFs. It is interesting to note that increasing solvent polarity from THF→MeOH→water, the morphology of the NMOF can be regulated among nanovesicle (**NMOF-1**) → nanoscroll (**NMOF-3**) → inverse-nanovesicle (**NMOF-2**). In control experiments, synthesized MOFs, using linker **1b** and **1c**, did not show any regular nanoscale morphology (Figure S19,S20), therefore, signifying the importance of mixed polar side chain for fabrication of vesicular NMOF with dynamic morphologies.

In order to study morphological flexibility and dynamicity with solvent polarity, **NMOF-1** (nanovesicle), synthesized in THF,

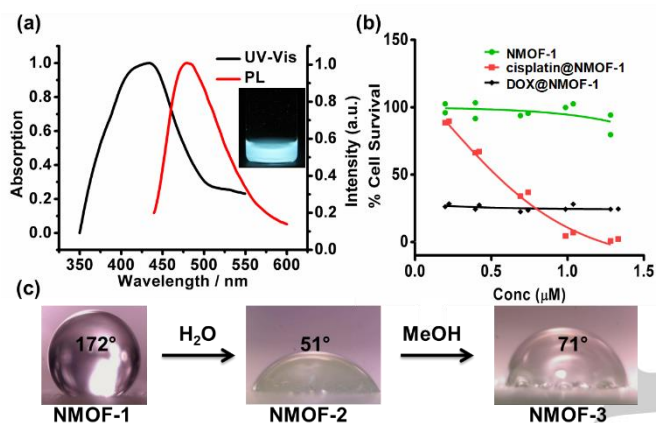


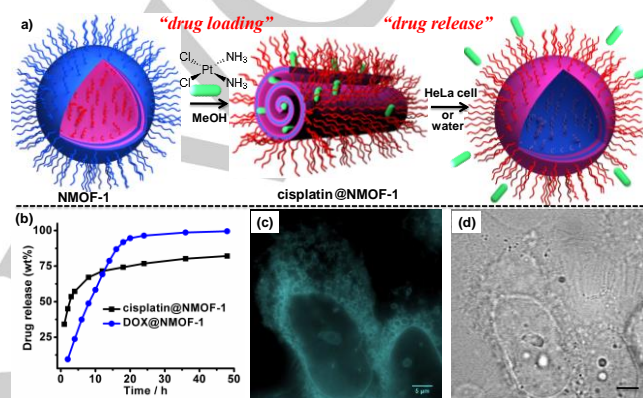
Figure 3. a) Normalized UV-Vis and PL spectra ($\lambda_{\text{ex}} = 433 \text{ nm}$) of **NMOF-1**. Inset: **NMOF-1** dispersion under UV light, b) cytotoxicity profile of **NMOF-1**, **cisplatin@NMOF-1** and **DOX@NMOF-1**. (c) Contact angle measurement of the transformed NMOFs.

was dipped in water for 3 h and the morphology was studied. FESEM images showed nanovesicular morphology and PXRD patterns (Figure S21,S22) were found to be similar to that of **NMOF-2**. In contrast, the measured water contact angle drastically dropped down to 51° from 172°, indicating hydrophilic outer surface decorated by TEG chains (Figure 3c, S23). Therefore, nanovesicle (**NMOF-1**) was converted to inverse-nanovesicle (**NMOF-2**) upon treatment with water. Similarly, **NMOF-2** was also converted to **NMOF-3** when dispersed in methanol and kept for 3 h. The transformation was supported by FESEM (nanoscroll morphology), PXRD and water contact angle (71°) measurement (Figure S23-S25). To understand the intermediate for **NMOF-2**→**NMOF-3** transformation, **NMOF-2** was charged in methanol for 1 h only and FESEM analysis revealed nanobelt morphology as an intermediate along with nanoscale semi-scrolls (Figure 2f). Dispersion of **NMOF-2** and **NMOF-3** in THF resulted in **NMOF-1** with superhydrophobic water contact angle of 156° and 162°, respectively (Figure S23/S26). Therefore, NMOF, synthesized from asymmetric bola-amphiphilic **1a** and Zn^{II} , showed solvent responsive dynamic shape and size shifting morphology transformation which is unprecedented in nanoscale MOF system.

All the NMOFs showed OPE based cyan emission with ~43% quantum yield (Figure 3a). **NMOF-1** was chosen for live cell imaging as it provides stable dispersion in different solvents (Figure 3a inset). Inherent emissive nature of the OPE backbone

allowed us to perform cellular uptake for bioimaging. We have tested the cell uptake by structured illumination microscopy (SR-SIM) after treating the HeLa cells with **NMOF-1**, suspended in DMEM culture media (0.2 mg ml^{-1}). The SR-SIM image of the cells, which was recorded after 48 h of incubation at 37 °C showed the presence of cyan emission from the cells, indicating efficient uptake of the **NMOF-1** by HeLa cell (Figure S27,S28).

The nanovesicular **NMOF-1** has surface decorated dodecyl chains and the inner TEG chains create hydrophilic cavity which can offer multiple H-bonding interactions toward encapsulation of cisplatin and doxorubicin drug molecules. Morphological flexibility of NMOF could also allow drug release by changing the solvent. As expected, cisplatin was successfully loaded into **NMOF-1**, from a saturated solution of



Scheme 4. a) Schematic representation of drug loading and release by NMOFs. b) Drug release profile of **cisplatin@NMOF-1** and **DOX@NMOF-1** in 1xPBS buffer. (c) SR-SIM image of HeLa cells after treatment with **cisplatin@NMOF-1** (scale bar: 5 μm).

methanol/water (v/v 11:1, SI), and the loading amount was quantified to be 14.4 wt% by detecting Pt in ICP and EDAX analyses (Figure S29). The TGA analysis of the **cisplatin@NMOF-1** showed an additional step of weight loss in the range 200-300 °C due to the early decomposition of cisplatin (Figure S30). FT-IR spectrum also revealed the presence of N-H stretching of the encapsulated cisplatin at 3283 cm^{-1} (Figure S31). Indeed, **cisplatin@NMOF-1** showed drastically reduced CO_2 uptake (195 K, $p = 1$) of 26.1 cc/g compared with **NMOF-1** (55.5 cc/g, Figure S32). The encapsulation also resulted in 20 nm blue-shift and 7 nm red-shift in the UV-Vis and PL maximum, respectively, further suggesting encapsulation of cisplatin within the **NMOF-1** (Figure S33). All these studies supported that cisplatin encapsulation occurred inside the vesicles. FESEM analysis of the **cisplatin@NMOF-1** showed nanoscroll morphology which is similar to **NMOF-3** (Figure S34). Moreover, elemental mapping revealed that the encapsulated cisplatin is distributed homogeneously into the nanoscroll (Figure S34). The in-vitro drug release was studied by dialysis and quantified by detecting Pt via ICP analysis (Figure 4b). In 1xPBS buffer (pH 7.4), 67% drug was released within 8 h and then release kinetics became slow providing 82% of drug release in 48 h. The kinetics was also found to be similar in 10xPBS (pH ~ 6.8, Figure S37). Absence of Zn^{II} in the solution is indicative of the structural integrity of the NMOF. We have tested the delivery potential of **cisplatin@NMOF-1** via HeLa cell culture studies (Figure 4c,d,S38-S40). The cells (~30,000 cells/100 μL culture medium)

COMMUNICATION

were incubated with different concentrations (20 μM to 1.25 μM) of **cisplatin@NMOF-1** and **NMOF-1** (control). PrestoBlue cell viability assay indicated that **cisplatin@NMOF-1** is very toxic with $\text{IC}_{50} \sim 0.5 \mu\text{M}$ (Figure 3b, S41-S43). The control experiments with only **NMOF-1** into cells showed no appreciable cytotoxic behavior thereby confirming the ability of the **NMOF-1** as an efficient payload carrier and delivery vehicle. Further, to study versatility of **NMOF-1** as a delivery vehicle, doxorubicin (**DOX**) was loaded in **NMOF-1** from THF medium. **NMOF-1** showed 4.1 wt% loading of **DOX** as confirmed from FT-IR, UV-Vis, TGA and elemental analysis (Figure S44-S46). PXRD analysis of **DOX@NMOF-1** showed the stability of the framework and drastic reduction in CO_2 uptake (55.5 cc/g \rightarrow 12.8 cc/g) indicating encapsulation of **DOX** inside **NMOF-1** (Figure S47, S48). The in-vitro drug release study in 1xPBS buffer exhibited 99% release of **DOX** within 48 h (Figure 4b, S49). Efficient payload delivery and corresponding cell death were also observed upon treating HeLa cells with **DOX@NMOF-1** (Figure 3b) indicating general applicability and versatility of the delivery vehicle.

Notably, the vesicular morphology and PXRD patterns of **NMOF-1** remained intact in DMEM culture media (Figure S50). The **NMOF-1** showed 3.3% and 18.8% hydrolysis in 1xPBS buffer and 10% FBS protein containing DMEM culture media after 10 days (Figure S51). **NMOF-C12** and **NMOF-OMe**, synthesized from the linker **1b** and **1c**, respectively, decomposed by 0.2% and 27.1%, respectively, in 1xPBS buffer after 10 days (Figure S52). This result indicated that the aqueous stability of **NMOF-1** originated due to the presence of dodecyl chains, possibly by reducing effective concentration of water molecules near the inorganic building unit.

In conclusion, synthesis and characterization of a solvent adaptive reversible shape-shifting luminescent nanoscale MOF have been successfully demonstrated. The adapted design principle for making such soft and smart material is based on the utilization of mixed polar side chains containing bola-amphiphilic OPE dicarboxylate linker and its self-assembly with Zn^{II} in solvents of different polarity. This dynamic and nontoxic NMOF has been exploited for bioimaging. Furthermore, the material has been exploited for anti-cancer drug loading and delivery in HeLa cell with micromolar cytotoxicity. This study would open up a path in designing flexible MOFs based on novel linker toward drug delivery vehicles and other biomedical applications. Thus, our findings could help in designing cargo that captures a targeted molecule and release of it upon external stimuli.

Acknowledgements

TKM is grateful to the DST, India (Project No. MR-2015/001019; TRC-DST/C.14.10/16-2724), and JNCASR for funding. TKM also acknowledges Life science research, education and training at JNCASR (BT/INF/22/SP27679/2018). We thank Dr. W. A.

Caliebe for assistance in EXAFS measurement at PETRAIII of DESY, Helmholtz Association (HGF), (beamline P64) supported by the DST.

Keywords: OPE • Nanovesicles • Nanoscroll • Inverse-nanovesicle • Drug delivery

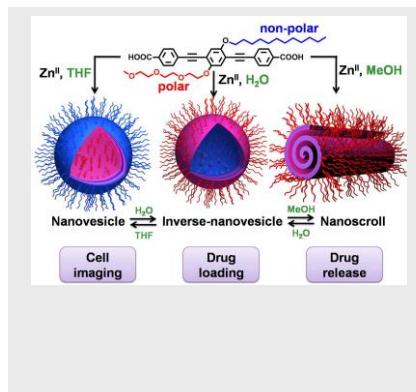
- [1] (a) K. J. Lee, J. H. Lee, S. Jeoung, H. R. Moon, *Acc. Chem. Res.* **2017**, *50*, 2684–2692; (b) C. Zhang, B. Wang, W. Li, S. Huang, L. Kong, Z. Li, L. Li, *Nat. Commun.* **2017**, *8*, 1138.
- [2] (a) Y. Li, J. Jin, D. Wang, J. Lv, K. Hou, Y. Liu, C. Chen, Z. Tang, *Nano Research*, **2018**, *11*, 3294–3305; (b) T. Simon-Yarza, A. Mielcarek, P. Couvreur, C. Serre, *Adv. Mater.* **2018**, *30*, 1707365; (c) T. Simon-Yarza, M. Giménez-Marqués, R. Mrimi, A. Mielcarek, R. Gref, P. Horcajada, C. Serre, P. Couvreur, *Angew. Chem. Int. Ed.* **2017**, *49*, 15565–15569; (d) M. Giménez-Marqués, T. Hidalgo, C. Serre, P. Horcajada, *Coord. Chem. Rev.* **2016**, *307*, 342–360; (e) T. Baati, L. Njim, F. Neffati, A. Kerkeni, M. Bouttemi, R. Gref, M. F. Najjar, A. Zakhama, P. Couvreur, C. Serre, P. Horcajada, *Chem. Sci.* **2013**, *4*, 1597–1607; (f) P. Horcajada, et al. *Nat. Mater.* **2010**, *9*, 172–178.
- [3] (a) K. Yuan, T. Song, D. Wang, Y. Zou, J. Li, X. Zhang, Z. Tang, W. Hu, *Nanoscale*, **2018**, *10*, 1591-1597; (b) M. Peller, K. Böll, A. Zimpel, S. Wuttke, *Inorg. Chem. Front.* **2018**, *5*, 1760-1779; (c) A. Carné, C. Carbonell, I. Imaz, D. Maspocho, *Chem. Soc. Rev.* **2011**, *40*, 291–305.
- [4] (a) P. Hirschle, T. Preiß, F. Auras, A. Pick, J. Völkner, D. Valdepérez, G. Witte, W. J. Parak, J. O. Rädler, S. Wuttke, *CrystEngComm*, **2016**, *18*, 4359-4368; (b) C. He, K. Lu, W. Lin, *J. Am. Chem. Soc.* **2014**, *136*, 12253–12256; (c) J. D. Rocca, D. Liu, W. Lin, *Acc. Chem. Res.* **2011**, *44*, 957-968;
- [5] (a) S. Wuttke, M. Lismont, A. Escudero, B. Rungtaweevoranit, W. J. Parak, *Biomaterials*, **2017**, *123*, 172-183; (b) B. Illes, P. Hirschle, S. Baerner, V. Cauda, S. Wuttke, H. Engelke, *Chem. Mater.* **2017**, *29*, 8042-8046; (c) R. Roder, T. Prei, P. Hirschle, B. Steinborn, A. Zimpel, M. Hohn, J. O. Radler, T. Bein, E. Wagner, S. Wuttke, U. Lachelt, *J. Am. Chem. Soc.* **2017**, *139*, 2359-2368; (d) P. Horcajada, et al. *Nat. Mater.* **2010**, *9*, 172–178.
- [6] (a) J. Cui, N. Gao, C. Wang, W. Zhu, J. Li, H. Wang, P. Seidel, B. J. Ravoo, G. Li, *Nanoscale*, **2014**, *6*, 11995-12001; (b) H. Xu, F. Liu, Y. Cui, B. Chen, G. Quian, *Chem. Commun.* **2011**, *47*, 3153–3155.
- [7] (a) M. M. Modena, P. Hirschle, S. Wuttke, T. P. Burg, *Small*, **2018**, *14*, 1800826; (b) C. Kong, H. Du, L. Chen, B. Chen, *Energy Environ. Sci.* **2017**, *10*, 1812-1819.
- [8] P. Horcajada, R. Gref, T. Baati, P. K. Allan, G. Maurin, P. Couvreur, G. Frey, R. E. Morris, C. Serre, *Chem. Rev.* **2012**, *112*, 1232–1268.
- [9] (a) S. Roy, D. Samanta, P. Kumar, T. K. Maji, *Chem. Commun.* **2018**, *54*, 275-278; (b) D. Samanta, P. Verma, S. Roy, T. K. Maji, *ACS Appl. Mater. Interfaces*, **2018**, *10*, 23140–23146; (c) S. Roy, V. M. Suresh, T. K. Maji, *Chem. Sci.* **2016**, *7*, 2251-2256; (d) V. M. Suresh, S. J. George, T. K. Maji, *Adv. Funct. Mater.* **2013**, *23*, 5585–5590.
- [10] (a) W. Schrimpf, J. Jiang, Z. Ji, P. Hirschle, D. C. Lamb, O. M. Yaghi, S. Wuttke, *Nature Commun.* **2018**, *9*, 1647; (b) R. Röder, T. Preiß, P. Hirschle, B. Steinborn, A. Zimpel, M. Höhn, J. O. Rädler, T. Bein, E. Wagner, S. Wuttke, U. Lächelt, *J. Am. Chem. Soc.* **2017**, *139*, 2359–2368. (c) T. Hidalgo, M. Giménez-Marqués, E. Bellido, J. Avila, M. C. Asensio, F. Salles, M. V. Lozano, M. Guillevic, R. Simón-Vázquez, A. González-Fernández, C. Serre, M. J. Alonso, P. Horcajada, *Sci. Rep.* **2017**, *7*, 43099.

COMMUNICATION

Table of Contents

COMMUNICATION

Solvent adaptive nanoscale MOF: A solvent adaptive reversible nanoscale MOF with dynamic morphology was devised based on an asymmetric bola-amphiphilic *oligo*-(*p*-phenyleneethynylene) (OPE) dicarboxylate linker. The emissive and non-toxic NMOF is cell permeable and allowed live cell imaging. Cisplatin (14.4 wt%) and doxorubicin (4.1 wt%) were encapsulated in the polar cavity of the NMOF and delivered to HeLa cell with micromolar cytotoxicity.



Debabrata Samanta, Syamantak Roy, Ranjan Sasmal, Nilanjana Das Saha, Pradeep K R, Ranjani Viswanatha, Sarit S. Agasti, Tapas Kumar Maji*

Page No. – Page No.

Solvent adaptive dynamic metal-organic soft hybrid for imaging and biological delivery